ISSN: 2093-5374 / E-ISSN: 2093-5382

Hybrid Deep Learning Model Based Lung Cancer Prediction and Classification with OTSU Segmentation Method

N. Muthu Bala[1*], and Dr.K.S. Kannan[2]

[1*]Assistant Professor, Department of Computer Science and Engineering, Dayananda Sagar University, Bengaluru, India. muthubala.phd@gmail.com, https://orcid.org/0009-0000-5172-5712

[2]Associate Professor, Department of Computer Science and Engineering, Kalasalingam Academy of Research and Education, Krishnankoil, Tamil Nadu, India. saikannan2012@gmail.com, https://orcid.org/0000-0002-1304-9829

Received: February 08, 2025; Revised: March 28, 2025; Accepted: May 05, 2025; Published: June 30, 2025

Abstract

The death rate for people diagnosed with Lung Cancer (LC) is rather high. Patients' lives may be saved if this illness is detected early and the stage of lung cancer is correctly identified. To determine whether a patient has lung cancer, traditional approaches use manual CT scans. This study presents a new approach to cancer cell segmentation and classification utilizing a Hybrid Deep Learning Neural Network (HDL) as a means of making an accurate and early diagnosis. What makes an HNN unique is its combination of the OTSU segmentation model with a Convolutional Neural Network (CNN) for feature extraction from CT image datasets and an enhanced LSTM: RNN classification model for improved classification accuracy. Prioritizing good health and well-being is essential for living a fulfilling and balanced life, enabling individuals to thrive both physically and mentally. The proposed method also makes it possible to distinguish between benign and cancerous tumors. We conducted a simulation experiment using the IQ-OTH/NCCD LC dataset and measured outcomes using the various performance metrics. According to the findings, the assessment criteria significantly reduce the classification time by around 50% while maintaining nearly the same classification impact. Based on the results of the simulations, our solution outperforms the classic classification algorithm in terms of convergence speed and time consumption, all while maintaining high classification accuracy. The study provides an attractive tool for quick image classification with great real-time performance.

Keywords: Lung Cancer, Segmentation, Classification, OTSU, Deep Learning, CNN, Good Health and Well-Being

1 Introduction

There is an immediate need to diagnose lung cancers at an initial stage to address disease since the number of cases has increased (Jones & Baylin, 2007; Nayak & Raghatate, 2024) (National Cancer Institute, 2021). Lung cancer survival rates and patient outcomes have improved due to advances in early detection and diagnosis (Worley, 2014). Among these methods, computed tomography (CT) scans have recently become an important resource for providing high-resolution images of the lung's internal

Journal of Wireless Mobile Networks, Ubiquitous Computing, and Dependable Applications (JoWUA), volume: 16, number: 2 (June), pp. 75-94. DOI: *10.58346/JOWUA.2025.I2.005*

*Corresponding author: Assistant Professor, Department of Computer Science and Engineering, Dayananda Sagar University, Bengaluru, India.

structure. Because it is so hard to diagnose, lung cancer has a long history of high fatality rates (Rani Saritha & Gunasundari, 2024; Dritsas & Trigka, 2022). The ability of CT scans to offer high-quality cross-sectional images of the lungs has allowed medical professionals and radiologists to identify tumors, suspicious lesions, and nodules at an unprecedentedly early stage (Iyer & Deshpande, 2024; Maurya et al., 2024). Improved deep-learning methods for effective LC prediction and classification have been developed due to this research. These methods use convolutional neural networks (CNNs) and GLCM-based feature extraction (Nasser & Abu-Naser, 2019; Zhou et al., 2017). The approaches CT and MRI are much more effective when DOST is used as an intermediary step. These modalities provide crucial details on the size, location, and extent of tumors. By supporting radiologists in interpreting complicated CT images, developments in computer-aided diagnosis (CAD) systems have increased the effectiveness as well as precision of LC classification (Mehra & Iyer, 2024). The challenge of reliably and precisely identifying lung cancer continues, even with current advancements (Sung et al., 2021; National Institutes of Health, 2021; Ferlay et al., 2021; Hegde & Chen, 2020). Because of the large number of CT images taken in medical settings, the fact that tumors might look somewhat different, and the importance of finding them early, reliable and effective automated methods are required. This is an area where deep learning algorithms have shown tremendous potential (Shekar et al., 2020).

Some of the most common and long-standing approaches for image segmentation consist of edge-based, region-based, and threshold-based employing gray histograms, among others. One of the various ways to segment images is by detecting changes in gray levels in the foreground and background. This works best when there is a clear difference between the colors of the foreground and background. Image contrast characteristics are not easily visible in real-world applications owing to issues such as uneven lighting; hence, several algorithms have limitations (Cerfolio et al., 2011). In contrast, the grayscale histogram-based threshold selection approach significantly enhances image segmentation performance by taking advantage of the image's overall grayscale properties. Specifically, Nobuyuki OTSU of Japan proposed a threshold image segmentation method called maximum inter-class variance that greatly enhances the image segmentation effect. This method uses the image's gray values to determine the extreme change between the foreground and background. However, a significant amount of computation is necessary. Considering that each variance takes T to compute, the overall variance calculation time for an image with 256 gray levels is 256 T, which lowers the image's segmentation effectiveness.

1.1 Motivation

Deep Learning (DL) has been steadily rising to the leading edge of computer vision research and development in recent years, with many academics turning to convolutional neural networks to tackle image classification issues (Zaidi & Chouvatut, 2023; Zhao et al., 2018). The majority of lung images are grayscale images, which are more detailed and have rich internal textures, but they are also more prone to imaging noise and machine interference, making identification much more challenging (Kourou et al., 2015). Manual feature extraction techniques, namely search trees, scale-invariant feature transformations, and orientation gradient histograms, are examples of traditional methods for extracting visual features (Tay et al., 2018). Unfortunately, when it comes to retrieving information from lung images, these low-level feature extraction approaches aren't very effective (Eo et al., 2012). Because of its great performance in computer vision and its ability to deliver high classification accuracy, CNN is normally used in image classification (Iyengar & Bhattacharya, 2024). Simultaneously, the attention mechanism has been recognized as a key component in enhancing classification ability. On the other hand, lung-classifying images aren't an ideal match for all attention processes and convolutional neural networks (Shi et al., 2024; Iwano et al., 2008). There has been an increase in studies on the topic of improving the clinical diagnosis rate of benign and malignant lung nodules. A potential use of radiomics in quantitative analysis of patient CT images was proposed. This might lead to a more precise diagnosis of benign and malignant pulmonary nodules as well as the identification of additional small lung lesions. Some typical methods for identifying lung images include cluster classification with two parameters, multispectral image classification, and iterative classification using pixel classification probability. The VGG class of networks introduced CNN to the mainstream, which has now spread to other domains. Because of its powerful ability to analyze deep image features, CNN has been used in several research for lung classification tasks. Typically, a CNN will have three layers: convolutional, pooling, and fully connected (Astaraki et al., 2021). To improve image feature extraction and classification accuracy, an increasing number of researchers are exploring deeper and larger networks. This causes the model's complexity to increase dramatically, which in turn raises the standard for what machines can do with data (Lu et al., 2020; Toraman et al., 2019).

1.2 Contribution

Traditional image processing methods' feature extraction algorithms' stability, variety of feature extraction algorithms and classifiers, and design complexity all work together to prevent the advancement of image segmentation algorithms (Surendar et al., 2024). Additionally, the network's capacity to retrieve feature information is constrained. This study's goal was to find ways to speed up image segmentation as well as classification with less computing cost and better accuracy. It offered several approaches that combined OTSU segmentation with CNN and LSTM-RNN.

To determine the optimal threshold for obtaining optimum separation features, the OTSU segmentation technique employs class discrimination. CT image segmentation often makes use of the OTSU method due to its ability to accurately preserve CT image features and edge information (Liu, 2011; Venkadesh et al., 2021). The simplicity and quickness of Otsu's approach are two of its numerous advantages. It can autonomously choose the finest threshold value to divide processed image's foreground and background areas without any previous knowledge of the image. Furthermore, it is compatible with bimodal histograms, a kind of data that is prevalent in many contexts. This research article proposes an OTSU segmentation model that uses a CNN for feature extraction and an LSTM-RNN model for deep-learning attention mechanisms based on image classification. The goal is to minimize model complexity while maintaining good classification accuracy. Improving classification accuracy requires a lightweight approach that focuses on important characteristics and regions of lung cancer images (Gang et al., 2018; Li et al., 2020; Agarwal & Patni, 2021; Selvanambi et al., 2020).

The objective of this research is to enhance patient outcomes by creating a reliable and effective early detection and classification system for lung cancer (Madhan & Shanmugapriya, 2024; Masud et al., 2020; Al-Yasriy et al., 2020; Javed et al., 2024; Krishna et al., 2024). The main goal of the proposed Hybrid Deep Learning Neural Network (HDL) is to minimize computation time when achieving high classification accuracy (Krizhevsky et al., 2012). It does this by integrating OTSU segmentation with a CNN for feature extraction and an upgraded LSTM-RNN model for classification. This methodology aims to distinguish between benign and malignant tumors, providing a reliable instrument for efficient image classification that outperforms conventional methods in real time (Barui et al., 2018; Naseer et al., 2022).

The main significant contributions of this research model are:

- Developing a DL approach for CT scan images to identify and classify lung cancer.
- OTSU segmentation, CNN feature extraction, and LSTM-RNN-based image classification are key components of the models.

- Assess the performance using different measures, such as F-Score, Specificity, Sensitivity, Accuracy, and Precision.

The outline of this document is as follows: Part II details the review of relevant research on the topic of lung cancer identification and classification. The methods employed in this proposed study are described in Section III. Chapter 4 delves into the specifics of the dataset, experimental setting, and performance evaluation of the results to those of previous studies on the same topic. Section V concludes this research work.

2 Related Work

Recent studies and research on medical imaging methods, deep learning algorithms, and lung cancer diagnosis will be covered in the literature review section (Rami-Porta et al., 2018). By analyzing and synthesizing this research, the review will provide the basis for the proposed hybrid deep learning approach and support its importance in improving LC diagnosis from lung CT input images.

In 2022, Dritsas et al. put out Rotation Forest, an algorithm that is noted for its great performance and is evaluated using popular metrics. Their 97.1% accuracy rate was rather remarkable. The study did not address the possible difficulties or restrictions of the Rotation Forest method, which is a drawback of the research. It developed a CNN with optimizers using the LUNA16 dataset, which includes data from different phases of lung nodules (Pavlopoulou et al., 2015). Despite this, they did reach an excellent accuracy of 97.42%. In their study, extracted features using an ensemble model are discussed. Afterward, these characteristics were pooled to serve as classification input. The method isn't perfect since they didn't provide about potential issues with the ensemble model. In, the author suggested a conventional CNN using the AlexNet Network Model for early tumor identification. Their study achieved an impressive 96% accuracy rate while using a private dataset. Nevertheless, this research has many limitations, one of which is that it relies on a private dataset. This might lead to bias and restrict the results' applicability to other datasets. In 2020, author reported a classification accuracy of 97.9% utilizing a light CNN architecture. One restriction, however, is that the research didn't test how well it worked on any other datasets; it just analyzed the LIDC dataset. In they have suggested a CNN method for cancer classification and detection by AlexNet (Iqbal et al., 2021) (Abbasi & Tajeripour, 2017). A disadvantage of using an unbalanced dataset is that it might lead to biased performance of models and lower efficacy in recognizing minority classes, even when their accuracy is 93.548%. I Fourier Transform Infrared (FTIR) spectroscopic signals were proposed by the author in. 2019. They succeeded in having a 95.71% efficiency rate (Katz & Bar-Ness, 2014).

To detect lung nodules, developed an ANN that achieved an accuracy of 96.67%. One shortcoming of this research is that it doesn't go into enough depth to address any problems or restrictions that may have arisen during the training and growth of ANNs. In 2018, they showcased a Glow-worm swarm optimization that achieved an impressive 98% accuracy. A limitation is that the research doesn't go into detail about the problems or difficulties that can arise from using the GSO algorithm to forecast lung cancer. They presented a CNN hybrid using networks such as LeNet and AlexNet. An accuracy percentage of 87.7 % was produced. Nevertheless, the study's lower-than-expected accuracy might be a cause for concern and affect the reliability and efficacy of the suggested hybrid CNN method.

Each study's strengths and limitations are summarized in Table 1. To sum up, lung cancer patients may have better results, reduced death counts, and higher lifetime with early diagnosis. Efforts to combat lung cancer must focus on this area because of the significant social and economic advantages it provides.

Table 1: Research Gap in Lung Cancer Detection and Classification

Reference	**Methodology**	**Accuracy Value**	**Cons**
(Jain et al., 2020)	LeNet & AlexNet	87.70%	Less accurate hybrid CNN techniques may affect reliability and efficacy.
(Ausawalaithong et al., 2018)	CNN with AlexNet	93.55%	Unbalanced data biases model performance and reduces minority efficacy.
(Abbasi & Tajeripour, 2017)	Glow-worm swarm optimization	98%	Insufficient mention of GSO algorithm limitations
(Luo et al., 2017)	CNN hybrid with AlexNet	96%	Private datasets can affect and restrict generalizability.
(Clark et al., 2013)	Ensemble model	94.5	Ensemble model limitations not discussed
(Weinstein et al., 2013)	Rotation Forest	97.10%	Not discussing the algorithm's drawbacks
(Luo et al., 2017)	Light CNN architecture	97.90%	Additional dataset performance unexplored
(Clark et al., 2013)	CNN with optimizers	97.42%	The training dataset is large
(Eo et al., 2012)	ANN	96.67%	Insufficient study or explanation of ANN development/training limitations/challenges

Diagnostic imaging modalities consisting of CT scans, X-rays, and MRIs may be better understood with the use of CAD systems (Shatnawi, Abuein & Al-Quraan, 2025). To analyze images and identify potential problem areas, these systems employ sophisticated algorithms in conjunction with hybrid deep learning approaches. Their goal is to make diagnostics more precise and faster. Limitations in processing include but are not limited to, image analysis's insufficient clinical context, the possibility of false negatives, and poor input image quality. Patients may benefit from the study's results in numerous ways: Enhanced surveillance and tracking, customized therapy methods, earlier detection and treatment, less complex actions, better quality of life, etc.

3 Proposed Methodology

The new, improved algorithm for lung cancer classification is illustrated in Figure 1, which is a block schematic of its process flow. Several essential parts make up the algorithm. The new Improved approach integrates pre-processing steps, OTSU Segmentation, CNN-based feature extraction, and LSTM: RNN for classification, to provide a summary. The goal of these procedures is to enhance the image, separate the lung sections, get the useful features, and finally use an LSTM: RNN with ranking features for precise LC detection. One thresholding approach that has been utilized for image segmentation is the Otsu method. To distinguish between pixels in the foreground and the background, it determines an "optimal" threshold value. The Otsu technique relies on maximizing the between-class variation to establish the threshold value, a critical parameter. Pixels can be classified as either foreground or background depending on their intensity levels using this threshold value. The classification process then makes use of the LSTM: RNN module.

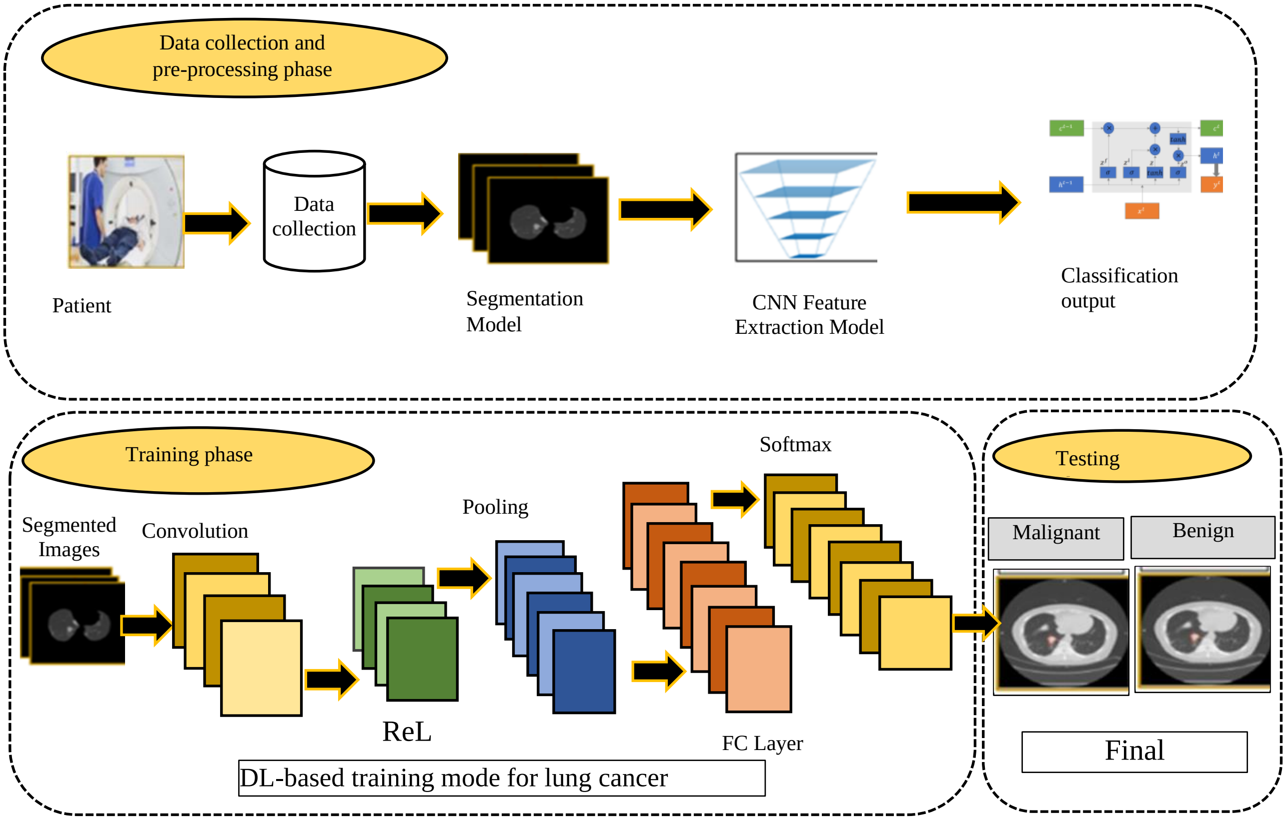

Figure 1: Implementation Flow of the Proposed Model for Lung Segmentation and Classification

3.1 OTSU Segmentation Model

The OTSU technique was proposed in 1979 by OTSU, a group of Japanese researchers, as a worldwide adaptation of the binarization-based threshold image segmentation system. As a criterion for selection, this method uses the highest interclass variance between the background and the target image. It uses the image's grayscale properties to classify it as either foreground or background. At the optimal threshold, the disparity between the two components is at its largest. The most often used metric in the OTSU method is the highest inter-class variance. A larger variance indicates a more pronounced dissimilarity between the two graph segments, which is relevant for assessing the degree to which data follows a uniform distribution. The disparity between the two components will decrease if certain backgrounds are mistakenly split into targets or vice versa. The greater the foreground-background inter-class variance, the more distinct the two components are from one another. The OTSU threshold value will be skewed toward the type with a large interclass variance when disparity between the two parts' interclass variances is large. This means that certain pixels in the kind of information with a large interclass variance will be put to a class with a smaller interclass variance, which leads to incorrect segmentation. The probability of incorrect classification is minimized when the inter-class variation is maximized using threshold value segmentation.

Here is a description of the fundamental basis of OTSU-based threshold segmentation given in Equation (1): N pixels compose an image if the grayscale range is $i = 0, 1, .., L-1$, and the number of pixels with a grayscale value of k is n_k.

$$N = \sum_{k=0}^{L-1} n_k = n_0 + n_1 + \cdots + n_{L-1} \tag{1}$$

Gray level $k's$ probability of occurring is given by Equation (2),

$$p_k = \frac{n_k}{N} = \frac{n_k}{\sum_{k=0}^{L-1} n_k} \tag{2}$$

The gray level threshold T has been used to segment an image into two clusters: $C_0 = (0,1,2,\ldots,t), C_1 = (t+1, t+2, \ldots, L_1)$. After dividing an image's gray level by the threshold T, we get $C_0 = (0,1,2,\ldots,t)$ and $C_1 = (t+1, t+2, \ldots, L-1)$, with the following probabilities in Equation (3-6) and means for the two classes:

$$w_0 = P_r(C_0) = \sum_{i=0}^{t} P_i = w(t) \tag{3}$$

$$w_1 = P_r(C_1) = \sum_{i=t+1}^{L-1} P_i = 1 - w(t) \tag{4}$$

$$u_0 = \sum_{i=0}^{t} \frac{iP_i}{w_0} = u_t/w(t) \tag{5}$$

$$u_1 = \sum_{i=t+1}^{L-1} \frac{iP_i}{w_1} = u_T - u_t/1 - w(t) \tag{6}$$

Among them, $u(t) = \sum_{i=0}^{L-1} iP_i, u_r = \sum_{i=0}^{L-1} iP_i$

$for\ all\ valurs\ of\ t,$

$w_0 u_0 + w_1 u_1 = u_T, w_0 + w_1 = 1$

You may use these formulae of Equation (7) and (8) to add up the variances of $C_0\ and\ C_1$:

$$\sigma_0^2 = \sum_{i=1}^{t} \frac{(i-u_0)^2 P_i}{w_0} \tag{7}$$

$$\sigma_1^2 = \sum_{i=1}^{t} (i-u_1)^2 P_i / w_1 \tag{8}$$

The variance for inter-class is given by Equation (9)

$$\sigma_W^2 = w_0 \sigma_0^2 + w_1 \sigma_1^2 \tag{9}$$

The variance for inter-class is given by Equation (10)

$$\sigma_B^2 = w_0 (u_0 + u_r)^2 + w_1 (u_1 + u_r)^2 = w_0 w_1 (u_1 - u_0)^2 \tag{10}$$

The inter- class variance for population is given by Equation (11)

$$\sigma_T^2 = \sigma_B^2 + \sigma_W^2 \tag{11}$$

Let consider the decision criteria on t:

$$\lambda(t) = \frac{\sigma_B^2}{\sigma_W^2}$$

$$\eta(t) = \frac{\sigma_B^2}{\sigma_T^2}$$

$$k(t) = \frac{\sigma_T^2}{\sigma_W^2}$$

Analysing the scenario, it becomes clear that the three criteria listed above are equivalent. As a group, they agree that the optimal threshold value t is the one that distinguishes between classes C_0 and C_1. Thus, $\lambda(t), \eta(t)\ and\ k(t)$ are acknowledged as the highest standard for assessment. For the simple reason that σ_W^2 represents second-order statistical features while σ_B^2 represents first-order properties. σ_B^2 and σ_W^2 depend on the threshold value t, but σ_T^2 is unrelated to t, using $\eta(t)$ as the criteria is the simplest way to determine the appropriate threshold value t^*, which is given in Equation (12):

$$t^* = \arg_{0 \le t \le L-1} max\eta(t) \tag{12}$$

It is clear from the above reasoning that the optimal value of the threshold t^* for t is when σ_B^2 is at its highest.

3.2 CNN based Feature Extraction

The data in the images was reduced, compressed, and changed using CNNs. Therefore, data matrices were converted into vectors by use of the Flatten layers. A shorter version of these was generated by the activation functions via data compression, which included coding and transformation. Furthermore, the features map's dimensionality was decreased by the convolution and pooling procedures layers. A features vector is the output of the algorithms running at this stage;

Regularized variants of CNN are multilayer perceptron. An information explosion might occur in these systems due to their interconnected nature. One major advantage of feature extraction is that it doesn't need any human intervention or previous knowledge. There are a number of ways to normalize or avoid overfitting. One is to decrease interconnectivity. Another is to compensate parameters during training. So, when it comes to complexity and connection, CNNs are significantly lower at the bottom.

A) CNN Layers

A CNN consists of five layers. The imaging data must be included in this CNN layer. Images are represented by a three-dimensional matrix. Transforming this layer into one continuous column is necessary. In order to supply an image with dimensions of 28 x 28 = 784, it first needs to be converted to 784 × 1.

B) CNN with Quai Gradient Descent

In order to calculate the local minimum or maximum of a function, one may use gradient descent (GD), a recurrent first-order optimization method. These methods are often used in ML and DL to decrease a loss function or cost. The two particular prerequisites of gradient descent are Differentiable and Convex.

Not all function satisfies the requirement that they are having a derivative at each point in their domain, but those that are spatially separated do. The line segment that connects various points on the function has to be on or above the univariate variable's curve in order for it to be considered convex. Equation (13) expresses this condition for two points x_1, x_2 on the function's curve.

$$f(\lambda x_1 + (1-\lambda)x_2) \leq \lambda f(x_1) + (1-\lambda)f(x_2) \tag{13}$$

where the value of λ, which represents the location of a point on a section line, should fall between 0 and 1. Half also indicates a middle ground. To determine whether a univariate function is convex, find out if the value of the second derivative has always been larger than zero.is given by Equation (14)

$$\frac{d^2f(x)}{dx^2} \tag{14}$$

C) Feature Extraction

The extraction models were created using CNN-based techniques using the following functions: VGG16 and VGG19. When designing the feature extraction layers, two primary considerations were proximity to the classifying layer and the results of experimental testing that took classification performance into account. The algorithms' selected layer types were:

- The VGG16 and VGG19 algorithms include a fully-connected layer called FC (Dense). In order to extracting features from images, this layer uses a 4096-dimensional feature vector;
- Flatten: EfficientNetB0's (EB0) block6d_add layer was subjected to this levelling layer of the methods VGG16 (VGG16 baseline) and VGG19 (VGG19 baseline). Data is transformed into a vector format by this layer. Vectors obtained using the VGG16 and VGG19 baseline approaches have 25088 dimensions. With respect to the EB0 function, the resulting vector has 9408 elements;

3.3 LSTM: RNN Classification Model

Technology that uses artificial intelligence to help physicians with diagnoses was introduced at the right time. Consequently, a DL approach based on attention mechanism is created to efficient classification of lung cancer image and reduce workload of medical applications. A RNN and LSTM are the building blocks of proposed model, which incorporates deep learning.

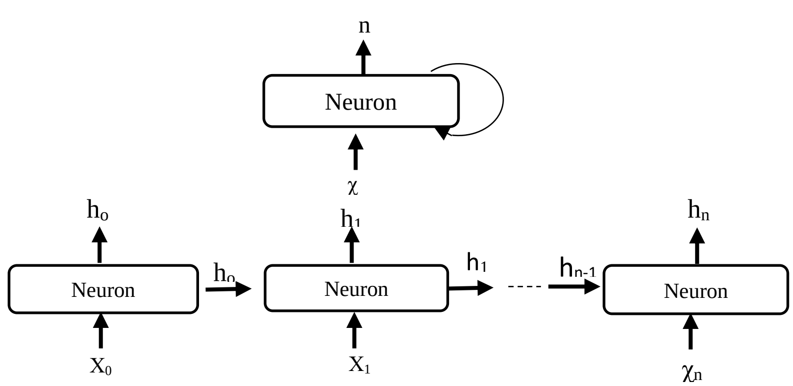

Figure 2: The Fundamental Architecture of RNN Model

An RNN is a model for processing sequence data that is based on deep neural networks. The fundamental aspect of this model is its ability to simulate data with variable length sequences by including the output of each neuron at time t into the input at the same time. Here is the fundamental layout of the network in Figure 2. One way to look at a neuron's output is as an encoded version of the subsequence that came before this one. Though other RNN neuron implementations exist, two prominent ones are LSTM and generalized recurrent units (GRU). Experimental findings from a comparison of GRU with LSTM and other recurrent neural networks on various sequence modelling tasks reveal that LSTM can outperform GRU while clearly benefiting from less training time.

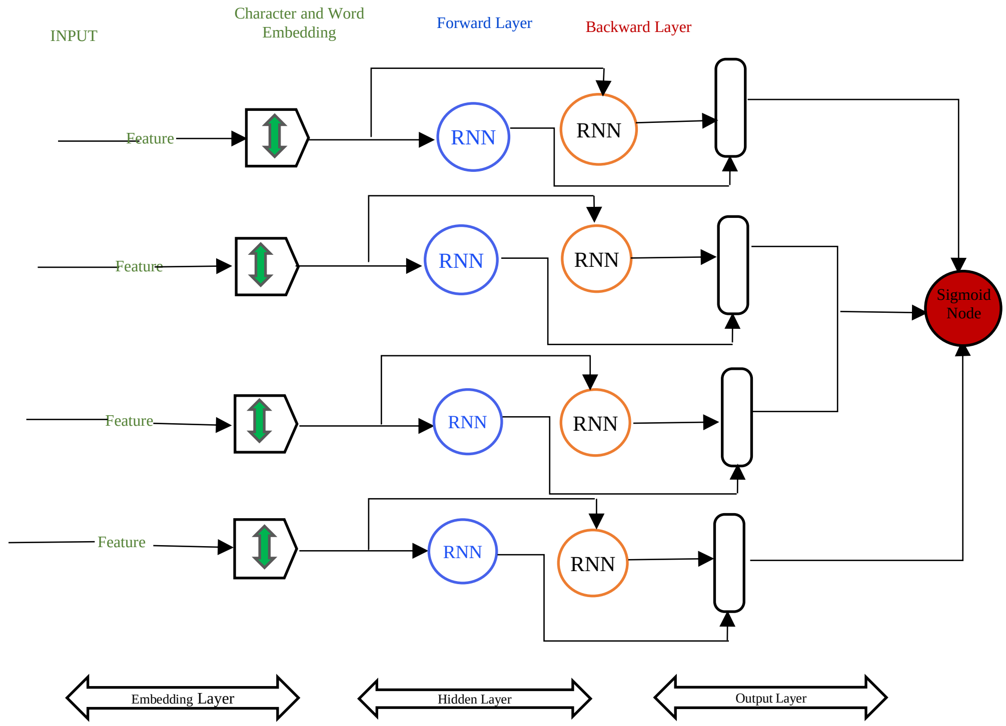

Figure 3: Illustration LSTM RNN Classification Model

Once the product is transferred to the attention module, it will do extensive data search and extraction using the extracted features. The last step in training a classifier to predict images is to flatten the acquired feature data into a one-dimensional feature vector. Figure 3 displays the block diagram of this model's general structure. In order to classify lung cancer using an LSTM-RNN model, medical images like X-ray or CT scans of the lung are analysed. The first step involves extracting and embedding characteristics from the input images, which transforms spatial data into numerical representations. A bidirectional LSTM (Long Short-Term Memory) network is used to process these properties. This kind of network analyses sequential input by mixing forward and backward layers, which allow it to record both past and future dependence. The LSTM-RNN is well-suited for detecting fine differences in medical data because to its exceptional ability to preserve long-term spatial and temporal patterns. In the final, classification layers are used to predict lung cancer based on the output from LSTM layers. By making good use of LSTM's capabilities, this design can reliably classify complicated medical imaging data.

Table 2: LSTM: RNN Structure Model

Input Size of image s	Step size	Convolution type
224*224*3	3*3*3*32	2D convolution
112*112*32	3*3*32	Depth wise Convolution
112*112*32	1*1*32*64	2D convolution
112*112*64	3*3*64	Depth wise Convolution
56*56*64	1*1*64*128	2D convolution
56*56*128	3*3*128	Depth wise Convolution
56*56*128	1*1*128*128	2D convolution
56*56*128	3*3*128	Depth wise Convolution
1*1*1024	1024*1000	fully connected layer
1*1*2	Classifier	classification layer

When choosing a model, this research stays away from the typical large-scale network approach. The deep learning lightweight network serves as foundational network for the experiment. A CNN is also a part of the main stage of feature extraction, and regular 2D convolution and convolution with depth-wise separable spacing are used for feature exploration. Both the training speed and the model's complexity have been decreased to some level in this approach. The LSTM-RNN network model's structural architecture is shown in Table 2.

4 Experimental Results and Discussion

4.1 Dataset Details

Data on lung cancer was gathered from the Iraq-Oncology Teaching Hospital/National Center for Cancer Diseases (IQ-OTH/NCCD). One hundred and ten cases' worth of CT scan slices (1,190 images overall) are included in the collection. There are three categories into which these instances fall: benign, normal, and malignant. Of them, 55 are deemed normal, 15 are deemed benign, and 40 have been classified as malignant. The information can be downloaded for free. Figure 4 displays the different lung images classified by disease.

Normal **Benign** **Malignant**

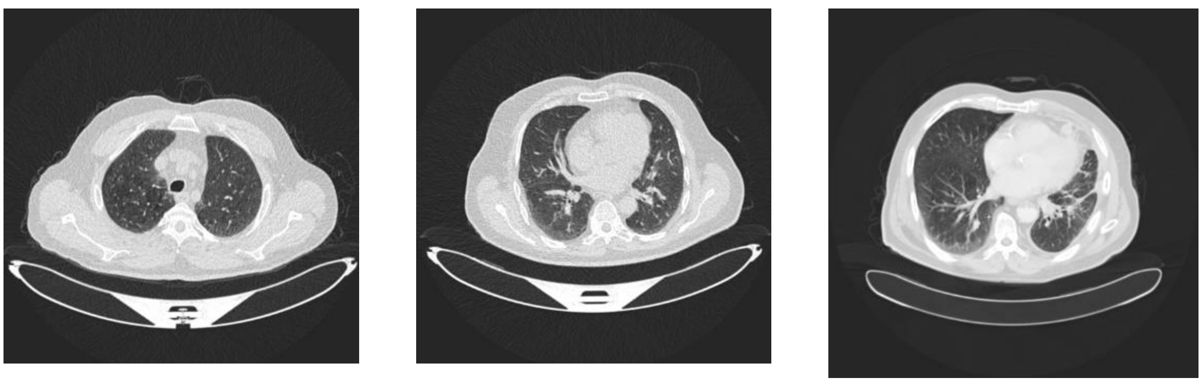

Figure 4: Samples of IQ-OTH/NCCD Lung Cancer Datasets

4.2 Evaluation Criteria

An objective metric for evaluating the segmentation algorithm's performance is the Signal-to-Noise Ratio (SNR) and the Peak Signal-to-Noise Ratio (PSNR). SNR is a measure for comparing estimated image to source image. The image quality improves as the value rises.

The SNR of a noise-contaminated image g (x,y) relative to a reference images f(x,y) is given by Equation (15):

$$SNR = 10 * log \frac{\frac{1}{MN} \sum_{x,y} f^2(x,y)}{\frac{1}{MN} \sum_{x,y} v^2(x,y)} = 10 * log \frac{\sum_{x,y} f^2(x,y)}{\sum_{x,y}\left(f(x,y) - g(x,y)\right)^2}$$

$$SNR = 10 \log_{10}\left[\frac{\sum_{x=1}^{M}\sum_{y=1}^{N} f^2(x,y)}{\sum_{x=1}^{M}\sum_{y=1}^{N}[g^2(x,y) - f^2(x,y)]^\wedge 2}\right] \tag{15}$$

PSNR is no more popular or commonly utilized image objective assessment index than this one. The image quality improves as the PSNR increases. Decibels (DB) are the units of measurement for PSNR. The formula is as given in Equation (16):

$$PSNR = 10 * \log \frac{255^2}{\frac{1}{MN} \sum_{x,y} v^2(x,y)} \; 10 * \log \frac{255^2}{MSE} \tag{16}$$

Typically, the formula for MSE expresses the anticipated value as square of discrepancy between the actual and estimated value. It stands for average of squares of the differences between the original and segmented pixel values in the image processing method.

An in-depth analysis of the tumor identification results at the demonstration stage was carried out using a confusion matrix. The results showed a percentage-based reliability for tumor prediction in metastases of different sizes. True Positive (TP), False Positive (FP), True Negative (TN), and False Negative (FN) are the four values used to calculate the confusion matrix. The Equation (17-22) is given the metric calculation formulae.

$$Accuracy = \frac{TP + TN}{TP + TN + FP + FN} \tag{17}$$

$$Precision = \frac{TP}{TP + FP} \tag{18}$$

$$Sensitivity = \frac{TP}{Tp + FN} \tag{19}$$

$$Specificity = \frac{TN}{TN + FP} \tag{20}$$

$$FPR = \frac{FP}{TN + FP} \tag{21}$$

$$F1 = 2 * \frac{TP}{2 * TP + FP + FN} \tag{22}$$

4.3 Performance Comparison on Segmentation Model

Table 3: Performance Comparison of Various Segmentation Model

Methods	**SNR (dB)**	**PSNR (dB)**
Fuzzy C Means	31.59	32.94
Thresholding	39.88	38.65
K-Means	41.82	40.85
OTSU	48.05	48.85

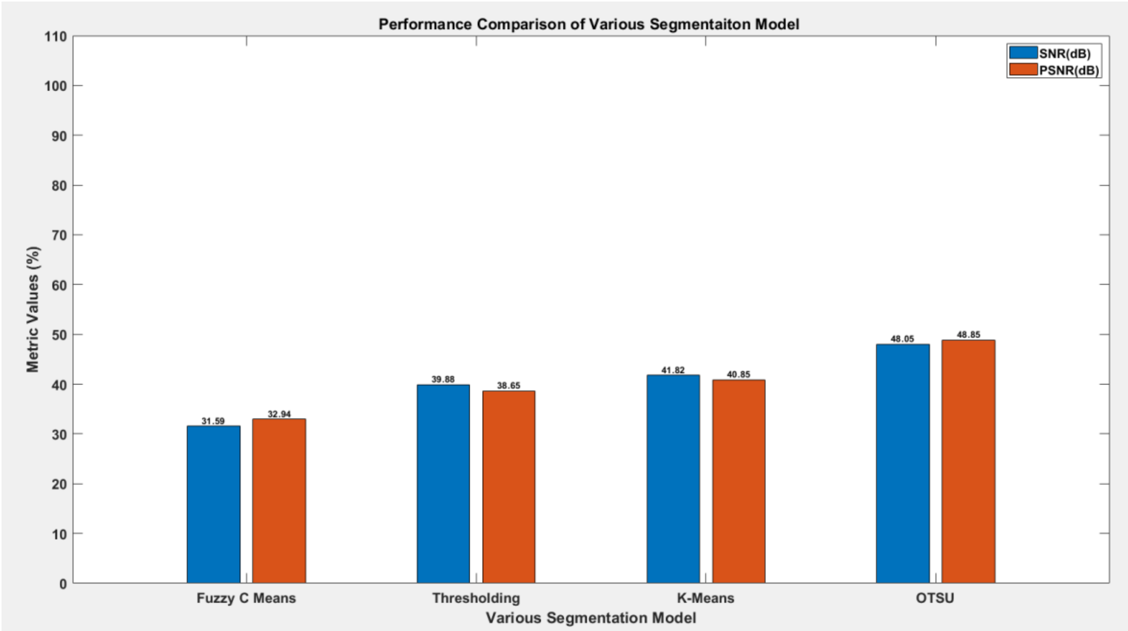

Figure 5: Performance Comparison of Various Segmentation Model

Based on the outcomes of the researches in Figure 5 (Table 3), it can be said that out of all the segmentation techniques, the OTSU approach achieved the highest SNR of 48.05 dB and PSNR of 48.85 dB. The thresholding segmentation approach achieved an accuracy of 38.65 dB, whereas K means clustering achieved a PSNR of 40.85 dB. It is also noted from the data that the FCM approach achieved a minimum accuracy level of 32.94 dB. Therefore, the OTSU segmentation approach ensures precise segmentation of the CT images of the lungs.

4.4 Model Validation on Feature Extraction

To ensure that stratified cross-validation is capable of generalizing classification models and to identify the optimal model for the provided dataset. The investigations used the confusion matrix, metrics for specificity, accuracy, sensitivity, and F1 score, together with their respective macro-averages, to assess effectiveness of proposed models for each cross-validation fold. Using mean F1 score as a benchmark, Table 4 compares the models' average performances across all macro-averages.

Table 4: Performance Comparison of Various Layer of CNN

CNN	Layer Type	Precision	Sensitivity	Specificity	F1 Score
Vgg16	FC	0.9811	0.9658	0.9732	0.9720
Vgg 16 baseline	Flatten	0.9757	0.9861	0.9806	0.9734
Vgg 19	FC	0.9874	0.9764	0.9854	0.9873
Vgg 19 baseline	Flatten	0.9654	0.9753	0.9774	0.9658

4.5 Performance Comparison on Classification Model

From the primary dataset, the training and testing datasets are separated in a 3:1 ratio, respectively. In Table 5 (Figure 6), we can see the results of running the different deep learning models on the given datasets.

Table 5: Performance Comparison of Classification Model

Parameters	LSTM: RNN	Inception V3	Resnet 50	VGG 16	VGG 19	CNN
Accuracy (%)	98.95	93.54	93.47	96.52	92.17	93.64
F-Score (%)	98.67	95.68	91.63	94.24	94.78	92.58
Specificity (%)	98.31	92.29	92.73	92.91	92.00	88.64
Precision (%)	97.85	90.57	93.31	92.14	91.46	89.76
Sensitivity (%)	98.57	91.73	91.14	93.71	93.20	91.70

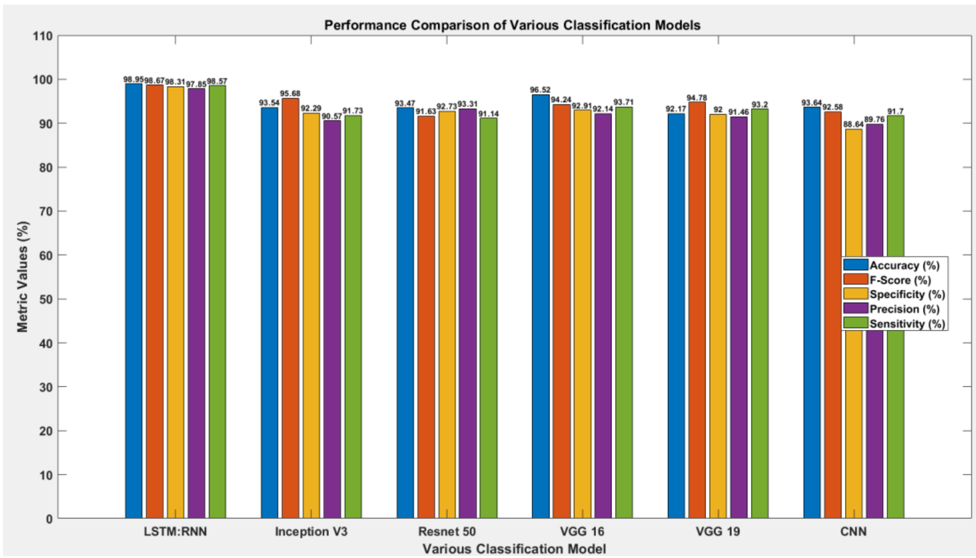

Figure 6: Performance Comparison of Various Classification Model for Lung Cancer Classification

There are six distinct models used to represent the results of the recognition accuracy analysis: LSTM: RNN, Resnet-50, VGG-16, Inception V3, and VGG-19. An improved accuracy of 98.95% is shown by the LSTM: RNN. In contrast to CNN's lesser precision of 89.76%, the LSTM: RNN model achieves a greater accuracy of 97.85%. With Resnet-50, the sensitivity rate is 98.57%, which is greater than the lower rate of 91.14%. While the lower rate is 88.64%, LSTM: RNN achieves the greatest specificity at 98.31%. Similarly, the highest F-Score achieved by LSTM: RNN is 98.67%, while the lowest F-Score for Resnet-50 is 91.63%. Using Convolutional Neural Networks (CNNs), LSTM: RNN, Inception V3, Resnet-50, VGG-16, and VGG-19, the proposed method detects lung cancer effectively. CNN models work well for recognizing and classifying images. When optimizing a CNN model, LSTM: RNN is the foundational algorithm that is utilized. One benefit of LSTM: RNN is that it uses training data to assist models develop over time. Although the training error % does not increase with Resnet's usage of a higher number of layers, the model is still readily trainable. When compared to current approaches, proposed model provides better accuracy, quicker training rates, and fewer training samples each iteration.

Because of its better ability to recognize complex sequences and long-term relationships in time-series data, LSTM-RNN attains the greatest accuracy in lung cancer classification. With the use of memory cells and gating mechanisms, LSTM-RNN is able to interpret images as multimodal inputs and provide more precise predictions. Because of its adaptability and resilience, the model outperforms competitors such as Inception V3, ResNet 50, and VGG architectures, even when presented with imperfect or noisy data. Thus, LSTM-RNN improves early detection and treatment planning by providing a holistic approach to lung cancer diagnosis.

4.6 Model Validation

The LSTM-RNN model is compared in Table 6 (Figure 7) with the basic CNN VGG16 and CNN VGG19 networks as feature extractors. The results are shown in terms of the overall accuracy (OA), the F1 score, and average precision (AP) on healthcare datasets (Sharma & Iyer, 2023). This approach achieves an OA accuracy of 97.68%, an F1 coefficient of 96.84%, and an AP accuracy of 96.67% according to the testing data. The fact that it outperforms the original basic network by 1.08%, 1.24%, and 1.04% as well as VGG16 and VGG19, demonstrates the efficacy of this approach. The proposed network shows reduced oscillation and quicker convergence compared to the deep learning network during model training. It is clear that the proposed approach is quite efficient as it can be used to classify lung images for public health and emergency medical emergencies very fast.

Table 6: Performance Comparison of OA, F1 and AP

Models	F1	OA%	AP%
LSTM-RNN	96.84	98.75	96.67
Inception-V3	92.85	92.85	93.12
VGG19	90.30	90.30	90.51
Deep learning	94.37	94.89	94.93
VGG16	95.06	94.38	94.36

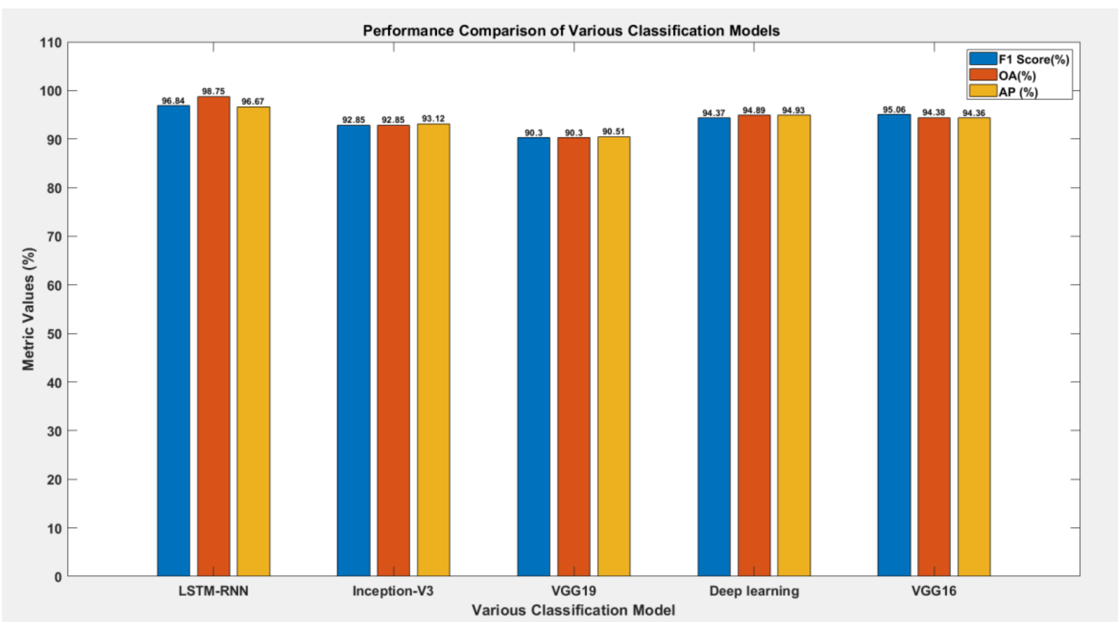

Figure 7: Performance Validation with Various Classification Model

4.7 Comparison with State of Art Models

The accuracy performance assessment of the proposed technique in contrast to prior methods utilized for lung cancer diagnosis is summarized in Table 7. A remarkable 99.269 % accuracy was attained by the proposed strategy. This level of accuracy shows that the proposed approach can accurately classify lung cancer patients, making it a powerful tool for identifying the illness. In addition to and the table also compares proposed models to others. When contrasted with pre-existing methods, which included both conventional ML and DL approaches, this shows that proposed approach considerably enhanced the accuracy of lung cancer diagnosis.

Table 7: Performance Comparison of State of Art Methods

Year	Techniques Used	Accuracy (%)
2020	CNN (Luo et al., 2017)	97.9
2021	Alexnet CNN (Ausawalaithong et al., 2018)	96
2022	CNN Alexnet +SGD (Clark et al., 2013)	97.42
2020	CNN with Alexnet (Luo et al., 2017)	93.458
2022	Machine Learning (Weinstein et al., 2013)	97.1
2019	ML with FTIR Signals (Tay et al., 2018)	95.71
2024	MLP (Astaraki et al., 2021)	89.29
2024	Logistic Regression Astaraki et al., 2021)	87.5
2023	Ensemble 2D CNN ((Barui et al., 2018)	95
Proposed Method (LSTM: RNN)		**98.75**

5 Conclusion and Future Work

In this study, we introduced HDL approach for the detection of lung cancer utilizing images of disease recovered from the IQ-OTH/NCCD database. Combining many image processing and analysis approaches, the proposed approach achieves reliable detection results. CNN for significant features in CT scans of lung cancer, OTSU segmentation has been used in proposed model. After that, an LSTM: RNN architecture learns these characteristics. In order to enhance classification performance, an increasing number of researchers are increasing the model's complexity by increasing the network's depth and breadth. This model enhances a lightweight network to investigate a CNN that is well-suited to extracting features from lung images, obtaining valuable information from these images, and minimizing the loss of important information. A high specificity of 99.1251%, sensitivity of 99.1121%, and total accuracy of 99.269% were shown by experimental findings, demonstrating the effectiveness of the proposed technique. The results of this work have important implications for the future of medical imaging using deep learning methods and for the precision with which lung cancer may be detected. This adds to the bigger image of medical research and practice and also has immediate consequences for patient treatment. The proposed technique has various direct consequences for clinical practice because to its high accuracy, specificity, and sensitivity: Better Results, Fewer False Positives, Quicker Treatment and an intervention, Better Use of Resources, Possibility of Screening Programs, and Improved Patient Satisfaction. This study's results might be useful for medical image analysis and lung cancer diagnosis in the future due to methods like Progress in Detection Methods, Incorporation of DL into Medical Imaging, Possibility of Transferable Methods, Impact on Research and Clinical Practice, Motivation for Additional Innovation. To further refine outcome, next study will use the RNN model based on metaheuristics for classification.

References

[1] Abbasi, S., & Tajeripour, F. (2017). Detection of brain tumor in 3D MRI images using local binary patterns and histogram orientation gradient. *Neurocomputing, 219*, 526-535. https://doi.org/10.1016/j.neucom.2016.09.051

[2] Agarwal, A., & Patni, K. (2021, July). Lung cancer detection and classification based on alexnet CNN. In *2021 6th international conference on communication and electronics systems (ICCES)* (pp. 1390-1397). IEEE. https://doi.org/10.1109/ICCES51350.2021.9489033

[3] Al-Yasriy, H. F., Al-Husieny, M. S., Mohsen, F. Y., Khalil, E. A., & Hassan, Z. S. (2020, November). Diagnosis of lung cancer based on CT scans using CNN. In *IOP conference series: materials science and engineering* (Vol. 928, No. 2, p. 022035). IOP Publishing. https://doi.org/10.1088/1757-899X/928/2/022035

[4] Astaraki, M., Zakko, Y., Dasu, I. T., Smedby, Ö., & Wang, C. (2021). Benign-malignant pulmonary nodule classification in low-dose CT with convolutional features. *Physica Medica*, *83*, 146-153. https://doi.org/10.1016/j.ejmp.2021.03.013

[5] Ausawalaithong, W., Thirach, A., Marukatat, S., & Wilaiprasitporn, T. (2018, November). Automatic lung cancer prediction from chest X-ray images using the deep learning approach. In *2018 11th biomedical engineering international conference (BMEiCON)* (pp. 1-5). IEEE. https://doi.org/10.1109/BMEiCON.2018.8609997

[6] Barui, S., Latha, S., Samiappan, D., & Muthu, P. (2018, April). SVM pixel classification on colour image segmentation. In *Journal of Physics: Conference Series* (Vol. 1000, No. 1, p. 012110). IOP Publishing. https://doi.org/ 10.1088/1742-6596/1000/1/012110

[7] Cerfolio, R. J., Bryant, A. S., McCarty, T. P., & Minnich, D. J. (2011). A prospective study to determine the incidence of non-imaged malignant pulmonary nodules in patients who undergo metastasectomy by thoracotomy with lung palpation. *The Annals of thoracic surgery*, *91*(6), 1696-1701. https://doi.org/10.1016/j.athoracsur.2011.02.075

[8] Clark, K., Vendt, B., Smith, K., Freymann, J., Kirby, J., Koppel, P., ... & Prior, F. (2013). The Cancer Imaging Archive (TCIA): maintaining and operating a public information repository. *Journal of digital imaging*, *26*(6), 1045-1057. https://doi.org/10.1007/s10278-013-9622-7

[9] Dritsas, E., & Trigka, M. (2022). Lung cancer risk prediction with machine learning models. *Big Data and Cognitive Computing*, *6*(4), 139. https://doi.org/10.3390/bdcc6040139

[10] Eo, Y. D., Pyeon, M. W., Kim, S. W., Kim, J. R., & Han, D. Y. (2012). Coregistration of terrestrial lidar points by adaptive scale-invariant feature transformation with constrained geometry. *Automation in Construction*, *25*, 49-58. https://doi.org/10.1016/j.autcon.2012.04.011

[11] Ferlay, J., Colombet, M., Soerjomataram, I., Parkin, D. M., Piñeros, M., Znaor, A., & Bray, F. (2021). Cancer statistics for the year 2020: An overview. *International journal of cancer*, *149*(4), 778-789. https://doi.org/10.1002/ijc.33588

[12] Gang, P., Zhen, W., Zeng, W., Gordienko, Y., Kochura, Y., Alienin, O., ... & Stirenko, S. (2018, March). Dimensionality reduction in deep learning for chest X-ray analysis of lung cancer. In *2018 tenth international conference on advanced computational intelligence (ICACI)* (pp. 878-883) IEEE. https://doi.org/10.1109/ICACI.2018.8377579.

[13] Hegde, P. S., & Chen, D. S. (2020). Top 10 challenges in cancer immunotherapy. *Immunity*, *52*(1), 17-35.

[14] Iqbal, M. J., Javed, Z., Sadia, H., Qureshi, I. A., Irshad, A., Ahmed, R., ... & Sharifi-Rad, J. (2021). Clinical applications of artificial intelligence and machine learning in cancer diagnosis: looking into the future. *Cancer cell international*, *21*(1), 270. https://doi.org/10.1186/s12935-021-01981-1

[15] Iwano, S., Nakamura, T., Kamioka, Y., Ikeda, M., & Ishigaki, T. (2008). Computer-aided differentiation of malignant from benign solitary pulmonary nodules imaged by high-resolution CT. *Computerized Medical Imaging and Graphics*, *32*(5), 416-422.

[16] Iyengar, S., & Bhattacharya, P. (2024). Assessing the Effects of Climate Change on Population Displacement and Migration Patterns in Coastal Communities. *Progression Journal of Human Demography and Anthropology*, 15-21.

[17] Iyer, R., & Deshpande, N. (2024). Nanotechnology and their Applications in Chiral and Achiral Separating Mechanisms. *Engineering Perspectives in Filtration and Separation*, 7-13.

[18] Jain, R., Nagrath, P., Kataria, G., Kaushik, V. S., & Hemanth, D. J. (2020). Pneumonia detection in chest X-ray images using convolutional neural networks and transfer learning. *Measurement*, *165*, 108046. https://doi.org/10.1016/j.measurement.2020.108046

[19] Javed, R., Abbas, T., Khan, A. H., Daud, A., Bukhari, A., & Alharbey, R. (2024). Deep learning for lungs cancer detection: a review. *Artificial Intelligence Review*, *57*(8), 197. https://doi.org/10.1007/s10462-024-10807-1.

[20] Jones, P. A., & Baylin, S. B. (2007). The epigenomics of cancer. *Cell*, *128*(4), 683-692. https://doi.org/10.1016/j.cell.2007.01.029

[21] Katz, E., & Bar-Ness, Y. (2014, November). Comparison of SNR and Peak-SNR (PSNR) as performance measures and signals for peak-limited two-dimensional (2D) pixelated optical wireless communication. In *2014 48th Asilomar Conference on Signals, Systems and Computers* (pp. 1880-1884). IEEE. https://doi.org/10.1109/ACSSC.2014.7094795

[22] Kourou, K., Exarchos, T. P., Exarchos, K. P., Karamouzis, M. V., & Fotiadis, D. I. (2015). Machine learning applications in cancer prognosis and prediction. *Computational and structural biotechnology journal*, *13*, 8-17. https://doi.org/10.1016/j.csbj.2014.11.005

[23] Krishna, S. U., Lakshman, A. N., Archana, T., Raja, K., & Ayyadurai, M. (2024). Lung cancer prediction and classification using decision tree and VGG16 convolutional neural networks. *The Open Biomedical Engineering Journal*, *18*(1). http://dx.doi.org/10.2174/0118741207290271240322061032

[24] Krizhevsky, A., Sutskever, I., & Hinton, G. E. (2012). Imagenet classification with deep convolutional neural networks. *Advances in neural information processing systems*, *25*.

[25] Li, X., Shen, L., Xie, X., Huang, S., Xie, Z., Hong, X., & Yu, J. (2020). Multi-resolution convolutional networks for chest X-ray radiograph based lung nodule detection. *Artificial intelligence in medicine*, *103*, 101744. https://doi.org/10.1016/j.artmed.2019.101744.

[26] Liu, S. (2011). Image segmentation technology of the ostu method for image materials based on binary PSO algorithm. In *Advances in computer science, intelligent system and environment* (pp. 415-419). Berlin, Heidelberg: Springer Berlin Heidelberg.

[27] Lu, Z. J., Qin, Q., Shi, H. Y., & Huang, H. (2020). SAR moving target imaging based on convolutional neural network. *Digital Signal Processing*, *106*, 102832. https://doi.org/10.1016/j.dsp.2020.102832

[28] Luo, Y., Wang, F., & Szolovits, P. (2017). Tensor factorization toward precision medicine. *Briefings in bioinformatics*, *18*(3), 511-514. https://doi.org/10.1093/bib/bbw026

[29] Madhan, K., & Shanmugapriya, N. (2024). Efficient Object Detection and Classification Approach Using an Enhanced Moving Object Detection Algorithm in Motion Videos. *Indian Journal of Information Sources and Services*, *14*(1), 9-16. https://doi.org/10.51983/ijiss-2024.14.1.3895

[30] Masud, M., Muhammad, G., Hossain, M. S., Alhumyani, H., Alshamrani, S. S., Cheikhrouhou, O., & Ibrahim, S. (2020). Light deep model for pulmonary nodule detection from CT scan images for mobile devices. *Wireless Communications and Mobile Computing*, *2020*(1), 8893494. https://doi.org/10.1155/2020/8893494

[31] Maurya, S. P., Sisodia, P. S., Mishra, R., & Singh, D. P. (2024). Performance of machine learning algorithms for lung cancer prediction: a comparative approach. *Scientific reports*, *14*(1), 18562. https://doi.org/10.1038/s41598-024-58345-8

[32] Mehra, A., & Iyer, R. (2024). Youth Entrepreneurship as a Catalyst for Inclusive Economic Growth in Developing Nations. *International Journal of SDG's Prospects and Breakthroughs*, *2*(3), 13-15.

[33] Naseer, I., Akram, S., Masood, T., Jaffar, A., Khan, M. A., & Mosavi, A. (2022). Performance analysis of state-of-the-art cnn architectures for luna16. *Sensors*, *22*(12), 4426. https://doi.org/10.3390/s22124426

[34] Nasser, I. M., & Abu-Naser, S. S. (2019). Lung cancer detection using artificial neural network. *International Journal of Engineering and Information Systems (IJEAIS)*, *3*(3), 17-23.

[35] National Institutes of Health. (2021). *Surveillance, Epidemiology, and End Results Program. Cancer stat facts: lung and bronchus cancer*. https://seer.cancer.gov/statfacts/html/lungb.html.

[36] Nayak, A., & Raghatate, K. S. (2024). Image segmentation and classification of aquatic plants using convolutional neural network. *International Journal of Aquatic Research and Environmental Studies*, *4*, 14-19. https://doi.org/10.70102/IJARES/V4S1/3

[37] Pavlopoulou, A., Spandidos, D. A., & Michalopoulos, I. (2015). Human cancer databases. *Oncology reports*, *33*(1), 3-18. https://doi.org/10.3892/or.2014.3579

[38] Rami-Porta, R., Call, S., Dooms, C., Obiols, C., Sánchez, M., Travis, W. D., & Vollmer, I. (2018). Lung cancer staging: a concise update. *European Respiratory Journal*, *51*(5). https://doi.org/10.1183/13993003.00190-2018

[39] Rani Saritha, R., & Gunasundari, R. (2024). Enhanced Transformer-Based Deep Kernel Fused Self Attention Model for Lung Nodule Segmentation and Classification. *Archives for Technical Sciences*, *31*(2), 175-191. https://doi.org/10.70102/afts.2024.1631.175

[40] Selvanambi, R., Natarajan, J., Karuppiah, M., Islam, S. H., Hassan, M. M., & Fortino, G. (2020). RETRACTED ARTICLE: Lung cancer prediction using higher-order recurrent neural network based on glowworm swarm optimization. *Neural Computing and Applications*, *32*(9), 4373-4386. https://doi.org/10.1007/s00521-018-3824-3

[41] Sharma, A., & Iyer, R. (2023). AI-powered Medical Coding: Improving Accuracy and Efficiency in Health Data Classification. *Global Journal of Medical Terminology Research and Informatics*, *1*(1), 1-4.

[42] Shatnawi, M. Q., Abuein, Q., & Al-Quraan, R. (2025). Deep learning-based approach to diagnose lung cancer using CT-scan images. *Intelligence-Based Medicine*, *11*, 100188. https://doi.org/10.1016/j.ibmed.2024.100188

[43] Shekar, G., Revathy, S., & Goud, E. K. (2020, June). Malaria detection using deep learning. In *2020 4th international conference on trends in electronics and informatics (ICOEI) (48184)* (pp. 746-750). IEEE. https://doi.org/10.1109/ICOEI48184.2020.9143023.

[44] Shi, S., Caluyo, F., Hernandez, R., Sarmiento, J., & Rosales, C. A. (2024). Automatic Classification and Identification of Plant Disease Identification by Using a Convolutional Neural Network. *Natural and Engineering Sciences*, *9*(2), 184-197. https://doi.org/10.28978/nesciences.1569560

[45] Sung, H., Ferlay, J., Siegel, R. L., Laversanne, M., Soerjomataram, I., Jemal, A., & Bray, F. (2021). Global cancer statistics 2020: GLOBOCAN estimates of incidence and mortality worldwide for 36 cancers in 185 countries. *CA: a cancer journal for clinicians*, *71*(3), 209-249. https://doi.org/10.3322/caac.21660

[46] Surendar, A., Veerappan, S., Sadulla, S., & Arvinth, N. (2024). Lung cancer segmentation and detection using KMP algorithm. *Onkologia i Radioterapia*, *18*(4).

[47] Tay, J. J., Wong, M. D., Wong, M. M., Zhang, C., & Hijazin, I. (2018). A tree search algorithm for low multiplicative complexity logic design. *Future Generation Computer Systems*, *83*, 132-143. https://doi.org/10.1016/j.future.2018.01.063

[48] Toraman, S., Girgin, M., Üstündağ, B., & Türkoğlu, İ. (2019). Classification of the likelihood of colon cancer with machine learning techniques using FTIR signals obtained from plasma. *Turkish Journal of Electrical Engineering and Computer Sciences*, *27*(3), 1765-1779. https://doi.org/10.3906/elk-1801-259

[49] Venkadesh, K. V., Setio, A. A., Schreuder, A., Scholten, E. T., Chung, K., W. Wille, M. M., ... & Jacobs, C. (2021). Deep learning for malignancy risk estimation of pulmonary nodules detected at low-dose screening CT. *Radiology*, *300*(2), 438-447. https://doi.org/10.1148/radiol.2021204433

[50] Weinstein, J. N., Collisson, E. A., Mills, G. B., Shaw, K. R., Ozenberger, B. A., Ellrott, K., ... & Stuart, J. M. (2013). The cancer genome atlas pan-cancer analysis project. *Nature genetics*, *45*(10), 1113-1120. https://doi.org/10.1038/ng.2764

[51] What Is Cancer? (2021). *National Cancer Institute*. https://www.cancer.gov/about-cancer/understanding/what-is-cancer.

[52] Worley, S. (2014). Lung cancer research is taking on new challenges: knowledge of tumors' molecular diversity is opening new pathways to treatment. *Pharmacy and Therapeutics*, *39*(10), 698.

[53] Zaidi, S. A., & Chouvatut, V. (2023). Mae Mai Muay Thai Style Classification in Movement Appling Long-Term Recurrent Convolution Networks. *Journal of Internet Services and Information Security*, *13*(1), 95-112. https://doi.org/10.58346/JISIS.2023.I1.010

[54] Zhao, X., Liu, L., Qi, S., Teng, Y., Li, J., & Qian, W. (2018). Agile convolutional neural network for pulmonary nodule classification using CT images. *International journal of computer assisted radiology and surgery*, *13*(4), 585-595. https://doi.org/10.1007/s11548-017-1696-0

[55] Zhou, W., Newsam, S., Li, C., & Shao, Z. (2017). Learning low dimensional convolutional neural networks for high-resolution remote sensing image retrieval. *Remote Sensing*, *9*(5), 489. https://doi.org/10.3390/rs9050489.

Authors Biography

N. Muthu Bala, is currently working as an Assistant Professor in Department of Computer Science and Engineering, School of Engineering at Dayananda Sagar university, Bangalore. She is pursuing her Ph.D in Kalasalingam Academy of Research and Education, deemed to be University, Krishnankovil, Tamil Nadu. She has 8 years of teaching experience. She has published 2 patents and 2 International/National Journals. She actively participated in more than 6 international and National Conference. Her areas of interest are Data Structures, Machine Learning, Deep Learning, Wireless Sensor Networks. She is a Life member in International Association of Engineers (IAENG), Hong Kong.

Dr.K.S. Kannan, is currently working as an Associate Professor in Department of Computer Science and Engineering, School of Computing at Kalasalingam Academy of Research and Education, deemed to be University, Krishnankovil, Tamil Nadu. His research interest is in the areas such as Machine Learning, Deep Learning, Computer Networks. He acted as reviewer in many journals. He has published more than 30 papers in National and International Peer Review Journals and Conferences and has 2 International Patent Granted and Published. He is presently supervising 6 Ph.D. Scholars, and has more than 20 years of teaching experience. He is a life member of ISTE.